

SAN097-0672C

CONF-970616 -- 7

COMPUTATIONAL CONTINUUM MODELING OF SOLDER INTERCONNECTS: APPLICATIONS*

S. N. Burchett

M. K. Neilsen

D. R. Frear

Sandia National Laboratories
Albuquerque, NM 87185-5800

RECEIVED

MAR 28 1997

OSTI

Abstract

The most commonly used solder for electrical interconnections in electronic packages is the near eutectic 60Sn-40Pb alloy. This alloy has a number of processing advantages (suitable melting point of 183C and good wetting behavior). However, under conditions of cyclic strain and temperature (thermomechanical fatigue), the microstructure of this alloy undergoes a heterogeneous coarsening and failure process that makes the prediction of solder joint lifetime complex. A viscoplastic, microstructure dependent, constitutive model for solder, which is currently under development, was implemented into a finite element code. With this computational capability, the thermomechanical response of solder interconnects, including microstructural evolution, can be predicted. This capability was applied to predict the thermomechanical response of a mini ball grid array solder interconnect. In this paper, the constitutive model will first be briefly discussed. The results of computational studies to determine the thermomechanical response of a mini ball grid array solder interconnects then will be presented.

Introduction

Solder joints were initially designed to be simple electrical interconnections between mechanically interlocked components in electronic packages. As technology advanced, electrical component size decreased, and the number of input/output terminations increased. To accommodate these changes, the number of solder joints per package has increased, while joint dimensions have decreased. The mechanically interlocked components were replaced by plated-through-hole technology which is now being pushed aside by surface mount technology (SMT). With each technological advance, the solder was expected to be not only an electrical conductor but also an increasingly important structural member with smaller and smaller feature size. The benefits of shrinking solder joint dimensions are numerous (e.g., increased speed, greater packing density, etc.) but reliability concerns increase substantially. A key issue of solder joint reliability is joint failure

due to thermal cycling since individual components that are soldered together in an electronic package have differing thermal expansion coefficients. Most current methodologies for evaluating and/or predicting solder joint reliability are empirically based. In these methodologies, specimens are manufactured, tested to failure for given sets of test conditions, and failure models are developed (usually based upon some form of Coffin-Manson relations). These failure models are then applied to similar geometries under different loading conditions to "predict" reliability. There are two major drawbacks to this methodology. First, substantial testing is required for each change such as geometry or material (e. g. lead free solder) and testing is expensive and time consuming. Second, it is difficult, if not impossible, to assess the effects of critical parameters on reliability through testing alone. To address these drawbacks, validated computational modeling is increasingly being used to assess solder joint response and reliability.

Computational modeling of solder interconnects is exceedingly difficult. To predict the thermal / structural response of any system, three elements must be defined; the geometry, the loading (including boundary conditions) and the material response (including failure). Solder interconnects present challenges in each of these elements. First, solder interconnects form during processing, therefore the local geometry of the solder interconnects will vary in size and shape, and may have imperfections. Additionally, the size of the solder interconnects are small relative to the package but are numerous. Therefore, obtaining the required resolution within the solder interconnects along with the required package geometry is computationally challenging. Second, the loading that can cause thermomechanical fatigue failure is essentially infinitely variable. Environmental thermal parameters such as temperature cycle range, hold times, and rates of temperature change can all affect solder interconnect reliability. Internal heating of electronic components can additionally affect reliability. Mechanical loading such as shock and vibration can affect reliability. Third, the material response of solder is exceedingly difficult to model computationally. Solder is a viscoplastic

*Sandia is a multiprogram laboratory operated by Sandia Corporation, a Lockheed Martin Company, for the United States Department of Energy under Contract Number DE-AC04-94AL85000.

MASTER

DISTRIBUTION OF THIS DOCUMENT IS UNLIMITED

12

DISCLAIMER

This report was prepared as an account of work sponsored by an agency of the United States Government. Neither the United States Government nor any agency thereof, nor any of their employees, make any warranty, express or implied, or assumes any legal liability or responsibility for the accuracy, completeness, or usefulness of any information, apparatus, product, or process disclosed, or represents that its use would not infringe privately owned rights. Reference herein to any specific commercial product, process, or service by trade name, trademark, manufacturer, or otherwise does not necessarily constitute or imply its endorsement, recommendation, or favoring by the United States Government or any agency thereof. The views and opinions of authors expressed herein do not necessarily state or reflect those of the United States Government or any agency thereof.

DISCLAIMER

Portions of this document may be illegible in electronic image products. Images are produced from the best available original document.

material in which the material parameters depend upon the microstructure. The initial microstructure depends upon processing, and the microstructure changes during thermomechanical loading. Additionally, even if the stress and strain response in solder can adequately be computed, predicting failure is a challenge.

Our laboratories efforts have focused upon the development of a viscoplastic, microstructurally dependent, constitutive model for solder. While this model is still being researched and developed, it shows promise to accurately predict the stress state, the evolution of the stress state with thermomechanical loading, and possibly provide a methodology to estimate the initiation of failure in solder interconnects. In this paper, the constitutive model will be briefly discussed. The constitutive model, at its present state of development, will then be applied to predict the thermomechanical response of a mini ball grid array (mbga) solder interconnect.

Internal State Variable Constitutive Model

A number of viscoplastic models have been developed for solder [1-5]. Several of these models include the initial grain or phase size as a material constant that does not change during the simulations. The viscoplastic model currently being developed is similar in many respects to the previous models; however, this new model incorporates grain size as an internal state variable which changes during the simulation. A scalar state variable is used to capture isotropic hardening and recovery and a second order state tensor is used to capture kinematic hardening and recovery. Coarsening is expected to have a significant effect on the state of the material, and a state variable which accounts for the reduction in flow stress with coarsening which follows the Hall-Petch relationship is included in the new model.

The proposed internal state variable model for solder has the following standard constitutive relation

$$\dot{\sigma} = \mathbf{E} : (\mathbf{d} - \mathbf{d}^{\text{in}}) \quad (1)$$

where $\dot{\sigma}$ is the Cauchy stress in the unrotated configuration, \mathbf{E} is the fourth-order, isotropic elasticity tensor, \mathbf{d} is the total deformation rate in the unrotated configuration, and \mathbf{d}^{in} is the inelastic deformation rate in the unrotated configuration [6]. The inelastic deformation rate is given by the following equation

$$\mathbf{d}^{\text{in}} = \frac{3}{2} \gamma \mathbf{n} = \frac{3}{2} f \exp\left(\frac{-Q}{R\theta}\right) \left(\frac{\lambda_0}{\lambda}\right)^p \sinh\left(\frac{\tau}{\alpha(c + \hat{c})}\right) \mathbf{n} \quad (2)$$

where g is the magnitude of the inelastic rate, f , p , m and Q are material parameters, R is the gas constant (1.987 cal/mole/K), q is the absolute temperature, l is the current grain diameter, l_0 is the initial grain diameter, a is a scalar function of the absolute temperature, and c and \hat{c} are state variables. \mathbf{n} is the normalized stress difference tensor which is given by,

$$\mathbf{n} = \frac{\mathbf{s} - \frac{2}{3} \mathbf{B}}{\tau} \quad (3)$$

where \mathbf{s} is the stress deviator, and \mathbf{B} is the state tensor which accounts for kinematic hardening. τ is a scalar measure of the stress difference magnitude,

$$\tau = \sqrt{\frac{3}{2} \left(\mathbf{s} - \frac{2}{3} \mathbf{B} \right) : \left(\mathbf{s} - \frac{2}{3} \mathbf{B} \right)} \quad (4)$$

Competing hardening and recovery mechanisms are captured by the evolution equations for the internal state variables c and \mathbf{B} . Evolution of the scalar state variable c is given by

$$\dot{c} = A_1 \gamma - (A_2 \gamma + A_3)(c - c_0)^2 \quad (5)$$

where c_0 , A_1 , A_2 , and A_3 are material parameters. Evolution of the second-order state tensor \mathbf{B} is given by

$$\dot{\mathbf{B}} = A_4 \mathbf{d}^{\text{in}} - (A_5 \gamma + A_6) \sqrt{\frac{2}{3} \mathbf{B} : \mathbf{B}} \mathbf{B} \quad (6)$$

where A_4 , A_5 , and A_6 are material parameters. The reduction in flow resistance with grain coarsening is captured by the scalar state variable \hat{c} . The state variable \hat{c} is related to the current grain diameter, l , by

$$\hat{c} = A_7 \left(\frac{\lambda_0}{\lambda} \right)^{A_8} \quad (7)$$

where A_7 and A_8 are positive material parameters, and l_0 is the initial grain diameter. Note that as the grain diameter, l , increases, \hat{c} decreases in magnitude which has the effect of reducing the flow resistance of the material. Evolution of the grain diameter, l , is given by the following equation

$$\dot{\lambda} = A_{11} \frac{(v_x + v_0)}{\lambda} \quad (8)$$

where A_{11} is a material parameter, v_x is the excess vacancy concentration and v_0 is the equilibrium vacancy concentration. Finally, the generation of excess vacancies due to inelastic deformation is given by

$$\dot{v}_x = A_9 \gamma - A_{10} v_x \quad (9)$$

where A_9 and A_{10} are material parameters.

This model was implemented into the finite element codes JAC2D [6], JAC3D [7], and JAS3D [8]. A complete description of the constitutive model development and implementation of the constitutive model into a finite element setting is the topic of a paper currently in preparation.

Applications

The currently implemented three-dimensional, time-dependent, viscoplastic, microstructural dependent capability was applied to predict the thermomechanical response of a single mini ball grid array (mbga) solder interconnect. The assumed three dimensional geometry of the mbga interconnect is shown in Figure 1. This geometry can be considered to be a solder interconnect at the outer extremity of the grid array. The substrate was assumed to be a ceramic material with a coefficient of thermal expansion (CTE) of $5 \times 10^{-6} \text{in/in}^\circ \text{C}$. The component was also assumed to be a ceramic material with a CTE of $6 \times 10^{-6} \text{in/in}^\circ \text{C}$. The CTE used for the solder was a handbook value of $25 \times 10^{-6} \text{in/in}^\circ \text{C}$. The initial microstructure of the solder was assumed to be uniform. The properties used for the viscoplastic solder model are given in Table 1. The substrate was assumed to be rigidly constrained

Table 1: Constants For 60/40 Solder

Property	Value
SHEAR MODULUS	1.72e6
BULK MODULUS	8.03e6
FLOW RATE	-0.287
SINH EXPONENT	10.40
GROWTH EXPONEN	3.00
ALPHA	1.00
BETA	1.00
A1	0.00
A2	0.00
A3	0.00
A4	3.26e5
A5	6.61e-2
A6	4.18e-6
A7	4455.0
A8	0.5
A9	1.00e-3
A10	16.6
A11	5.81e-5
FLOW STRESS	2500.
GRAIN SIZE	35.4e-6
VACANCY CONCEN	1.00e-9

and a symmetry boundary condition was applied to the front surface. A uniform time-dependent temperature history was applied. Simultaneously, a time-dependent displacement was applied to the component with magnitude of the applied displacement corresponding to the thermal expansion difference between the component and substrate assuming that the distance from the center of the component to the edge of the mbga interconnect was 0.46 inch (this corresponds to an average shear strain of 0.83%). The applied uniform temperature histories used in these computations are shown in Figure 2 and the applied displacement history is shown in Figure 3. The response of the solder interconnect was computed for six complete thermomechanical cycles. In Figure 4, the computed shear force (resultant load) is plotted as a function of time. This plot clearly shows the time-dependent creep response at high temperature and essentially elastic response at low temperature. In Figure 5, the computed shear force is plotted as a function of temperature. This plot shows the characteristic hysteresis

loops and starts to show the effect of microstructural changes on the response. In Figure 6, contours of the accumulated plastic strain in the solder interconnect at the end of six complete cycles is plotted. This plot indicates that the highest magnitude accumulated plastic strains are at opposite corners of the solder interconnect with the peak being at point A. In Figure 7, contours of the computed microstructural coarsening parameter in the solder interconnect at the end of six complete cycles is plotted. This plot also indicates that the highest magnitude of microstructural coarsening is also at opposite corners of the solder interconnect with the peak also being at point A. Experimental observations suggest that these locations are the initiation sites for solder interconnect cracking.

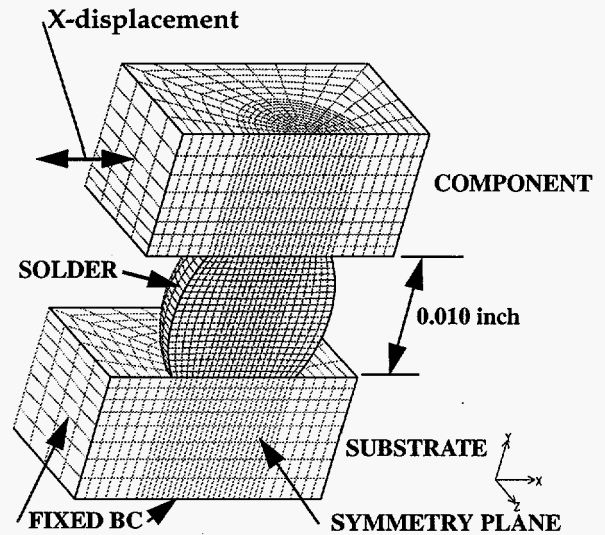


Figure 1. Geometry of Mini Ball Grid Array Solder Interconnect

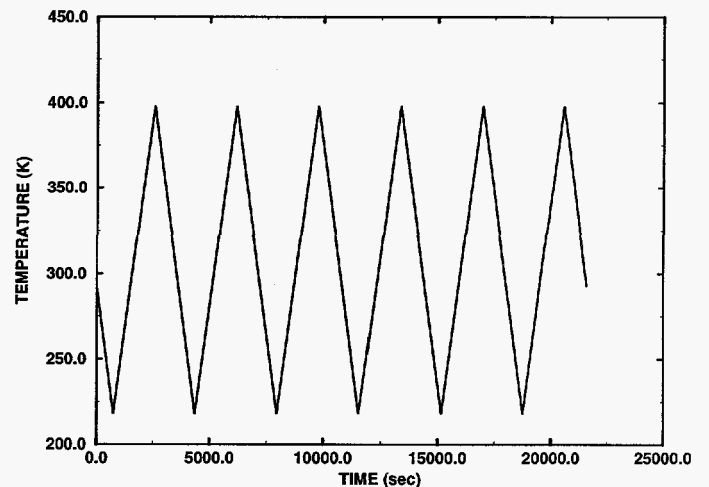


Figure 2. Applied Thermal Loading History

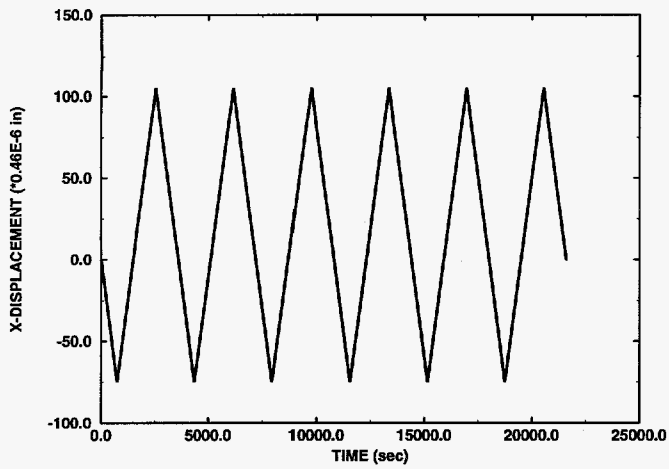


Figure 3. Applied Displacement History

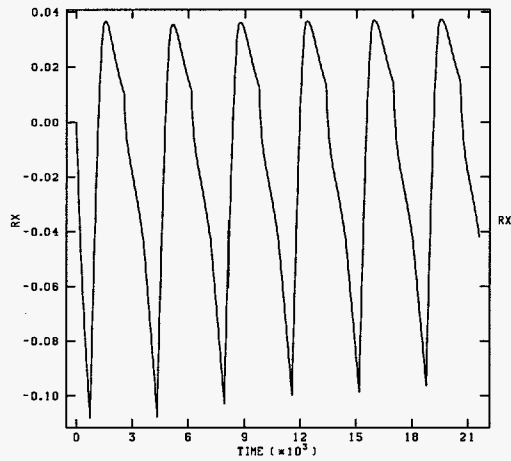


Figure 4. Computed Shear Force vs. Time

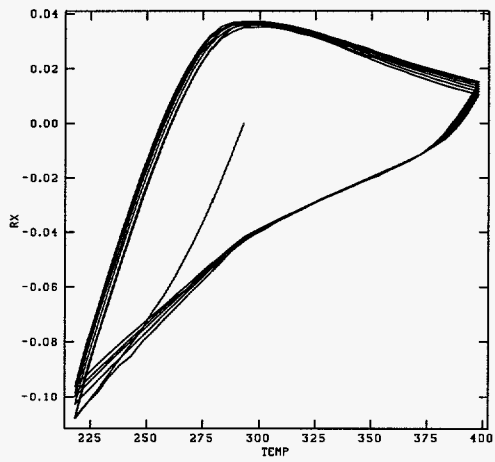


Figure 5. Computed Shear Force vs. Temperature

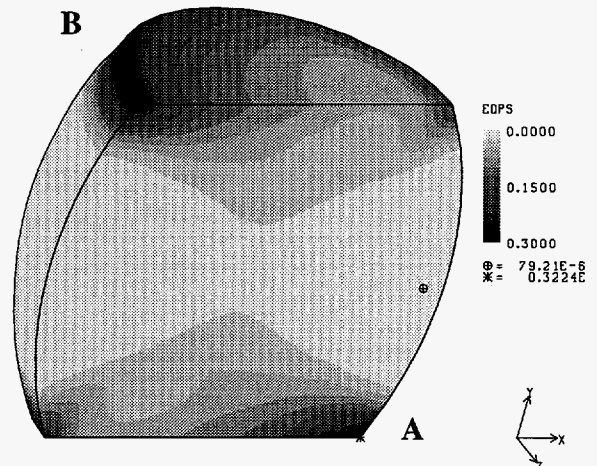


Figure 6. Computed Accumulated Plastic Strain @ 6 Cycles

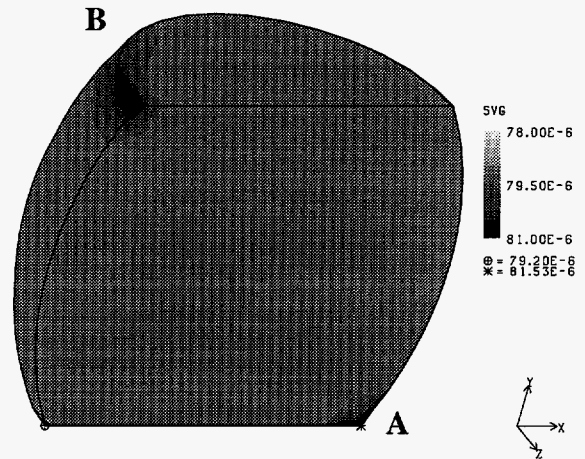


Figure 7. Computed Microstructural Parameter @ 6 Cycles

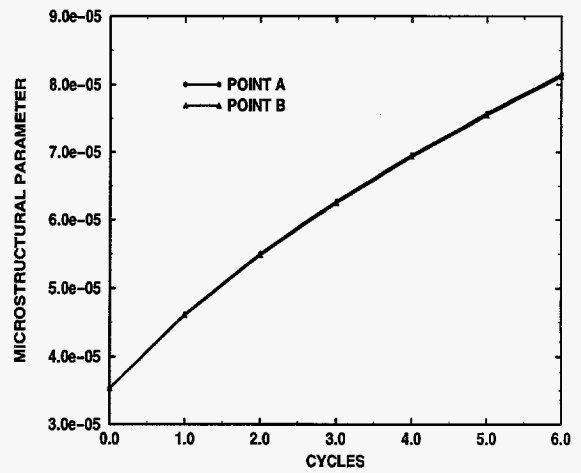


Figure 8. Computed Microstructural Parameter vs Time

Discussion

In Figure 8, the computed microstructural coarsening parameter at points A and B are plotted as a function of number of thermomechanical cycles. The microstructural coarsening parameter at Point A is only slightly larger than the microstructural coarsening parameter at point B. This would suggest that cracking would initially start at point A. The microstructural coarsening parameter can be considered to be a "damage" parameter which is the basis for developing a methodology for predicting lifetime. The initial methodology is to simply assume that when the microstructural coarsening or "damage" parameter reaches a critical value cracking initiates. Further research is needed to relate the magnitude of the "critical damage parameter" to initial cracking. Additionally, since the finite element computations are compute intensive, methodologies need to be developed to accelerate the computations or to extrapolate the results from a relatively few thermomechanical load cycles.

Summary and Conclusions

In this paper, the viscoplastic, microstructural dependent constitutive model currently being developed was briefly discussed. The model, which was implemented into a 3D finite element code, was applied to predict the thermomechanical response of a single mini ball grid array solder interconnect. While this model is still being researched and developed, the computational capability shows promise to accurately predict the stress state, the evolution of the stress state with thermomechanical loading, and possibly provide a methodology to estimate the initiation of failure in solder interconnects. Additional research will focus on obtaining accurate model parameters, developing a crack initiation criteria so that cycles to failure can be predicted, and accelerating the computations.

References

- 1) Akay, H. U., Y. Tong, N. Paydar, 1992, "Thermal Fatigue Analysis of an SMT Solder Joint Using FEM Approach", J. Microcircuits and Electron. Packaging, vol. 116, pp. 79-88.
- 2) Pan, T.-Y, W.L. Winterbottom, 1990, "Thermal Cycling Induced Plastic Deformation in Solder Joints", ASME Winter Annual Meeting, Dallas TX.
- 3) Hacke, P., A. F. Sprecher, H. Conrad, 1993, "Computer Simulation of Thermomechanical Fatigue of Solder Joints Including Microstructural Coarsening", ASME J. Electronic Packaging, vol. 115, pp. 153-158.
- 4) Busso, E. P., M. Kitano, and T. Kumazawa, 1992, "A Visco-Plastic Constitutive Model for 60/40 Tin-Lead Solder Used in IC Package Joints," J. Engr. Mater. Tech., Vol. 114, July 1992.
- 5) Guo, Z., A. F. Sprecher, and H. Conrad, 1992, "Plastic Deformation Kinetics of Eutectic Pb-Sn Solder Joints in Monotonic Loading and Low-Cycle Fatigue," J. Electronic Packaging, Vol. 114, June 1992.
- 6) Biffle, J. H. and M. L. Blanford, "JAC2D - A Two-Dimensional Finite Element Computer Program for the Non-Linear Quasi-Static Response of Solids with the Conjugate Gradient Method," SAND93-1891, Sandia National Laboratories, May 1994.
- 7) Biffle, J. H., and M. L. Blanford, "JAC3D - A Three-Dimensional Finite Element Computer Program for the Non-Linear Quasi-Static Response

of Solids with the Conjugate Gradient Method," SAND87-1305, Sandia National Laboratories, Febr. 1993.

- 8) Blanford, M. L., "JAS3D - A Multi-Strategy Iterative Code for Solid Mechanics Analysis - Release 1.3", Sandia National Laboratories, Febr. 1993.